

Representation-Regularized Convolutional Audio Transformer for Audio Understanding

Bing Han^{1*}, Chushu Zhou^{1,2*}, Yifan Yang¹, Wei Wang¹,
Chenda Li¹, Wangyou Zhang¹ and Yanmin Qian^{1†}

¹Auditory Cognition and Computational Acoustics Lab, Shanghai Jiao Tong University

²Shanghai Innovation Institute

{hanbing97, zhouchushu, yanminqian}@sjtu.edu.cn

Abstract

Bootstrap-based Self-Supervised Learning (SSL) has achieved remarkable progress in audio understanding. However, existing methods typically operate at a single level of granularity, limiting their ability to model the diverse temporal and spectral structures inherent in complex audio signals. Furthermore, bootstrapping representations from scratch is computationally expensive, often requiring extensive training to converge. In this work, we propose the Convolutional Audio Transformer (CAT), a unified framework designed to address these challenges. First, to capture hierarchical audio features, CAT incorporates a Multi-resolution Block that aggregates information across varying granularities. Second, to enhance training efficiency, we introduce a Representation Regularization objective. Drawing inspiration from generative modeling, this auxiliary task guides the student model by aligning its predictions with high-quality semantic representations from frozen, pre-trained external encoders. Experimental results demonstrate that CAT significantly outperforms baselines on audio understanding benchmarks. Notably, it achieves competitive performance on the AudioSet 20k dataset with 5 times faster convergence than existing methods. Codes and checkpoints will be released soon at <https://github.com/realzhouchushu/CAT>.

1 Introduction

Self-supervised learning (SSL) has become a cornerstone of representation learning, enabling models to extract meaningful patterns from unlabeled data across various modalities. In the audio domain, SSL has successfully mitigated the reliance on large-scale manual annotations, producing transferable representations for downstream tasks. Among these, bootstrap-based approaches, which employ a teacher-student framework to predict latent representations—have shown remarkable efficacy. State-of-the-art (SOTA) models such as data2vec series [Baevski *et al.*, 2022; Baevski *et al.*, 2023],

EAT [Chen *et al.*, 2024], ATST [Li *et al.*, 2024] and M2D [Nizumi *et al.*, 2024a] leverage this paradigm to achieve impressive results in audio understanding tasks.

Despite these advancements, current bootstrap-based audio SSL methods face two critical limitations. First, they often overlook the inherent hierarchical nature of audio signals. Audio events span diverse temporal and spectral scales, ranging from transient acoustic textures to long-term semantic contexts. Existing methods typically process audio at a single, fixed level of granularity, limiting their ability to capture these multi-scale structures effectively. Second, training these models from scratch is inherently inefficient. Relying solely on internal consistency between the teacher and student networks requires extensive computational resources and prolonged training periods to bootstrap high-quality representations from random initialization.

To address the efficiency bottleneck, we draw inspiration from recent advances in generative modeling, REPA [Yu *et al.*, 2025]. These studies demonstrate that generative models (e.g., diffusion models [Ho *et al.*, 2020; Song *et al.*, 2021]) converge significantly faster and generate higher-quality content when guided by representations from pre-trained encoders. We argue that the core objective of bootstrap SSL, predicting masked representations is fundamentally an implicit generative task. Just as diffusion models benefit from perceptual guidance, the “reconstruction” process in SSL can be accelerated by leveraging external semantic knowledge. Instead of learning solely from scratch, the student model can benefit from “standing on the shoulders of giants” by aligning with mature representations from external models.

Guided by this insight, we propose the Convolutional Audio Transformer (CAT), a unified framework designed to enhance both the granularity and efficiency of audio representation learning. To tackle the granularity issue, CAT incorporates a Multi-resolution Block. Unlike traditional single-layer patch embeddings, this module utilizes hierarchical convolutional layers to extract and aggregate features at multiple temporal and frequency scales, aligning with the multi-scale characteristics of audio signals. Simultaneously, to improve training efficiency, we introduce a Representation Regularization objective. We treat the student branch as a generative generator and align its intermediate features with high-quality representations from frozen, well-pretrained external encoders (e.g., CLAP [Wu *et al.*, 2023], Audio-MAE [Huang

*Equal Contribution †Corresponding Author

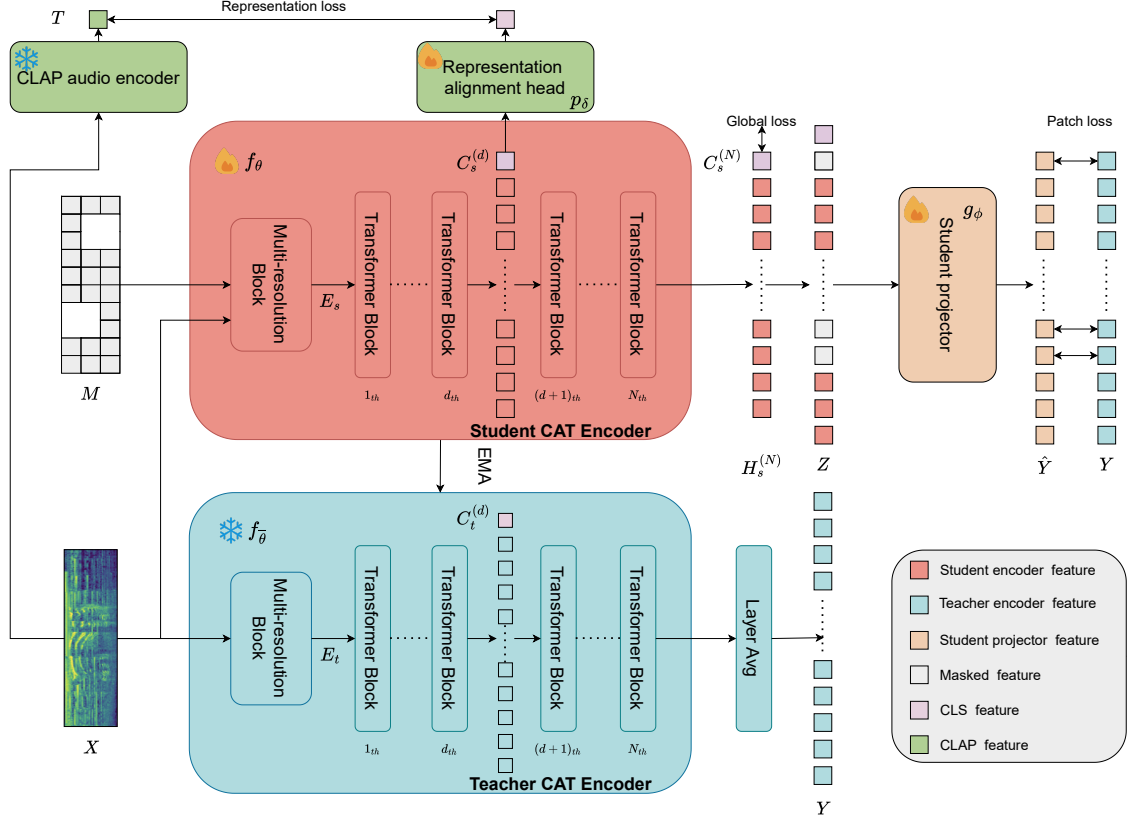


Figure 1: **CAT Pre-training Architecture Overview.** The model follows a student-teacher bootstrap paradigm. The Student Encoder processes a masked spectrogram, while the Teacher Encoder (updated via Exponential Moving Average, EMA) receives the unmasked input. The training objective is composed of three parts: (1) Patch-level Loss (L_p): The student projector predicts the teacher’s latent representations for masked patches; (2) Global Loss (L_g): Aligns the global CLS token of the student with the teacher’s aggregated features; (3) Representation Loss (L_r): A regularization term that aligns intermediate representations from the student encoder with high-quality features extracted from a frozen external audio encoder.

et al., 2022], AST [Gong et al., 2021a]). This auxiliary task provides stable semantic guidance, effectively “shortcutting” the early stages of representation learning.

Our experimental evaluations on audio and speech datasets validate the effectiveness of this approach. CAT not only achieves superior performance on audio understanding tasks compared to existing baselines but also demonstrates remarkable efficiency, highlighting the power of combining multi-resolution processing with representation regularization.

Our main contributions are summarized as follows:

- We propose the Convolutional Audio Transformer (CAT), which replaces the standard patch embedding with a Multi-resolution Block to capture audio information across varying granularities.
- We introduce Representation Regularization to audio SSL, formulating the masked prediction task as a generative process guided by external pre-trained encoders. This strategy significantly improves representation quality and training stability.
- We demonstrate that CAT establishes new state-of-the-art (SOTA) results on standard audio understanding

benchmarks with 5 times training speed-up.

2 Related Work

2.1 Pre-trained Audio Encoder

Supervised pre-training, contrastive pre-training and self-supervised pre-training are the three widely adopted approaches for audio encoder pre-training. Supervised pre-training usually relies on collected labels to guide model training. Representations extracted from supervised learning methods such as PANN [Kong et al., 2020], AST [Gong et al., 2021a] and HTS-AT [Chen et al., 2022a] perform well on various tasks. For contrastive pre-training, CLAP [Wu et al., 2023] consists of dual encoders—one for audio and one for text—trained jointly to align audio representations with their corresponding natural language descriptions. However, these methods typically require large amounts of labeled data, which limits their scalability. Self-supervised learning (SSL) methods have recently gained more attention, as they can learn high-quality representations while eliminating the need for labeled data. Some self-supervised methods including MAE-AST [Baade et al., 2022], Audio-MAE [Huang et

al., 2022] and MaskSpec [Chong *et al.*, 2023] follow the fashion of MAE [He *et al.*, 2022], using features of unmasked patches to predict masked audio patches. Another popular type of methods is bootstrap-based self-supervised methods. These approaches such as data2vec [Baevski *et al.*, 2022], EAT [Chen *et al.*, 2024] and A-JEPA [Fei *et al.*, 2023] adopt a student-teacher framework where the student model learns to predict representations generated by a slowly updated teacher model. Bootstrap-based self-supervised methods have demonstrated promising performance on various audio understanding tasks.

2.2 Representation Learning as Auxiliary Tasks

Beyond traditional training paradigms, recent studies in generative modeling have explored using external representations to guide the learning process. In the domain of image generation, REPA [Yu *et al.*, 2025] demonstrated that diffusion models—which generate images from noise—converge significantly faster when their intermediate features are regularized to align with representations from pre-trained encoders (e.g., DINOv2 [Oquab *et al.*, 2024]). Subsequent works have extended this concept: iREPA [Singh *et al.*, 2025] emphasizes the importance of spatial structural information, SARA [Chen *et al.*, 2025a] introduces multi-level representation alignment to optimize the diffusion training process and accelerate convergence, SoftREPA [Lee *et al.*, 2025] applies it to multimodal text-to-image generation, and Semantic-VAE [Niu *et al.*, 2025] utilizes alignment to enhance speech synthesis quality. We draw a parallel between these generative tasks and bootstrap-based SSL. We argue that the core objective of Masked SSL—predicting masked representations from partial inputs—is effectively an implicit generative task. Despite this theoretical connection, its potential to accelerate convergence and improve feature quality in understanding tasks (e.g., audio classification) remains underexplored. Our work bridges this gap by integrating representation regularization into the SSL framework, leveraging diverse external pre-trained encoders to provide additional guidance for efficient audio understanding.

3 Method

3.1 Model Architecture Overview

CAT is a pre-trained model following the bootstrap paradigm, similar to established methods such as data2vec [Baevski *et al.*, 2022], DINO [Oquab *et al.*, 2024] and EAT [Chen *et al.*, 2024]. The model architecture of CAT is illustrated in Fig. 1. CAT employs a dual-branch architecture encompassing a student model and a teacher model. The student model contains a CAT encoder f_θ followed by a projector module g_ϕ , while the teacher model solely consists of a CAT encoder $f_{\bar{\theta}}$. Although the student and teacher encoders share an identical architecture, they do not share parameters. This asymmetric design, with the projector only on the student side, effectively prevents representation collapse (i.e., the encoder outputting constant representations regardless of the input data).

During pre-training, CAT takes an audio spectrogram $\mathbf{X} \in \mathbb{R}^{T \times F}$ as input, where T and F denote the time and frequency

dimensions, respectively. The model employs two sets of hyperparameters: resolution parameters r_1, r_2, \dots, r_{n_r} and feature channel dimensions D_1, D_2, \dots, D_{n_r} , where n_r is the number of layers in the multi-resolution block, with each r_i ($i = 1, \dots, n_r$) specifying a distinct non-overlapping patch size for the i -th resolution layer, while D_i denotes the number of feature channels in the corresponding layer. Let P denote the total number of patches, where $P = TF/r_{n_r}^2$. In the teacher branch, the encoder $f_{\bar{\theta}}$ processes the entire spectrogram through a multi-resolution block, which subsequently outputs a feature representation $\mathbf{E}_t \in \mathbb{R}^{P \times D_{n_r}}$ that integrates information from multiple granularities. A comprehensive description of how the multi-resolution block works is provided in 3.2. Then, a learnable CLS token is added to this feature sequence for global representation learning. This representation is then fed into a stack of transformer blocks to further capture contextual dependencies. We denote the output of the j -th transformer block as $\mathbf{H}_t^{(j)}$ for the teacher branch and $\mathbf{H}_s^{(j)}$ for the student branch ($j = 1, \dots, N$), where N is the number of transformer blocks.

The student and teacher models share an identical encoder architecture but differ slightly in their input processing. For the teacher encoder, the target Y is derived from a mean-pooling operation over the hidden states of its internal layers.

$$\mathbf{Y} = \sum_{i=1}^N \frac{\mathbf{H}_t^{(i)}}{N} \quad (1)$$

For the student encoder, the student multi-resolution block takes an additional mask as input $\mathbf{M} \in \mathbb{R}^{P \times D_{n_r}}$. This mask is applied to the patchified spectrogram, yielding features \mathbf{E}_s . To enhance training efficiency, only the features corresponding to these unmasked patches are processed and output by the transformer blocks. After obtaining the output $\mathbf{H}_s^{(N)}$ from the final transformer block, pad embeddings are interpolated at the positions of the masked patches to form the projector input \mathbf{Z} . The projector g_ϕ comprises a sequence of lightweight convolutional layers. The feature \mathbf{Z} is then fed into the student projector g_ϕ , which outputs $\hat{\mathbf{Y}}$ that serves as the prediction of the output of the teacher encoder \mathbf{Y} .

3.2 Convolutional Audio Transformer Encoder

The CAT encoder comprises a multi-resolution block for extracting features at different granularities, followed by a stack of N transformer blocks. As shown in Fig. 2, The multi-resolution block contains n_r resolution blocks.

For the teacher CAT encoder, The first block takes the spectrogram $\mathbf{X} \in \mathbb{R}^{T \times F}$ as input. The output of the k -th resolution block, denoted as $\mathbf{E}_t^{(k)} \in \mathbb{R}^{\frac{T}{r_k} \times \frac{F}{r_k} \times D_k}$, serves as the input to the subsequent $(k+1)$ -th block for $k = 1, \dots, n_r - 1$. Given $\mathbf{E}_t^{(k)}$, the $(k+1)$ -th resolution block extracts coarser-grained features using a patch embedding module, which is implemented as a convolutional layer with a stride and kernel size of r_{k+1}/r_k . This feature is then passed through a subsequent convolution module composed of several lightweight convolutional layers, which are designed to further integrate information while preserving the shape of the feature, yield-

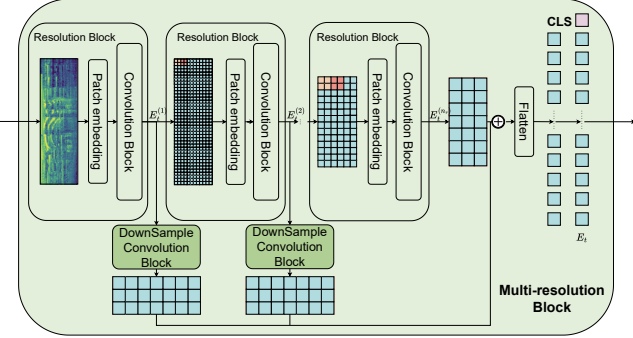


Figure 2: **Multi-Resolution Block Architecture.** This diagram depicts the data flow in the teacher’s Multi-Resolution Block. The student branch follows a nearly identical process, differing primarily by the introduction of an input mask that is element-wise multiplied with the features inside the Convolutional Block.

ing the output $E_t^{(k+1)}$. Since the output shapes of the different resolution blocks vary, several additional downsample blocks are introduced to project each intermediate representation $E_t^{(k)}$ to the same shape as the final output $E_t^{(n_r)} \in \mathbb{R}^{\frac{T}{r_{n_r}} \times \frac{F}{r_{n_r}} \times D_{n_r}}$. The downsampled outputs are summed together and then flattened. Subsequently, a learnable classification (CLS) token is added to the beginning of this sequence to form the final integrated representation E_t .

The student CAT encoder is almost identical to the teacher encoder, with the key difference that it accepts an additional mask M as input. This mask is interpolated and reshaped to match the spatial dimensions of each intermediate feature $E_s^{(k)}$, and is then applied to the features within the convolutional block. Another difference is that, for the student CAT encoder, all features corresponding to masked patches are removed, retaining only the unmasked features before these features are finally passed into transformer blocks to reduce computation.

3.3 Training Objective with Representation Regularization

Representation regularization has demonstrated promising performance on generative tasks. Benefiting from the asymmetric structure of CAT, we argue that the student branch (the student CAT encoder together with the student projector) is an implicit generative model. The key difference is that the target domain of its generation is not raw images or raw audio signals, but the teacher model’s representations corresponding to the masked patches. Introducing representation regularization as an auxiliary task may improve the student model’s generation performance (e.g., leading to better alignment with the teacher), and therefore enhance the representation learning quality of the encoder. Furthermore, guided by well-trained external representations, the training process can be easier compared with relying solely on the model to learn representations independently from scratch.

Motivated by this, we introduce representation regularization as an auxiliary task optimized jointly with the original

main objective. The overall objective L can be defined as:

$$L = L_p + \lambda_1 L_g + \lambda_2 L_r \quad (2)$$

where L_p and L_g are the patch-level loss and global loss in the original main objective, and L_r is the representation learning loss used for representation regularization. λ_1 and λ_2 are hyperparameters manually assigned as the loss weights of L_g and L_r .

We align the intermediate representations of our model with those extracted by an external model by introducing a representation learning loss L_r . Specifically, we feed the unmasked audio into a frozen pre-trained encoder such as CLAP [Wu *et al.*, 2023] to extract representations $T \in \mathbb{R}^{1 \times D_t}$, which are then used as the target. A single-layer representation alignment head p_δ operates on the CLS token of the d -th student transformer block (d is a hyperparameter), mapping its feature dimension from D_{n_r} to D_t . The L_r can be given by:

$$L_r = \left\| p_\delta(C_s^{(d)}) - T \right\|_2^2 \quad (3)$$

This strategy encourages the model to learn global semantic information that is invariant to patch masking while providing meaningful guidance to accelerate convergence.

The original training objectives are retained following the setting of Data2vec [Baevski *et al.*, 2023]. To compute the patch-level loss L_p , the student projector takes the unmasked patch features $H_s^{(N)}$ from the student encoder and outputs \hat{Y} to predict the teacher encoder’s outputs Y for both masked and unmasked patches. L_p is computed only over the masked patches, formulated as the Mean Squared Error (MSE) between the prediction and the target:

$$L_p = \left\| \hat{Y}_{\text{masked}} - Y_{\text{masked}} \right\|_2^2 \quad (4)$$

To capture the global audio representation, we use the CLS token from the final student transformer output $C_s^{(N)} \in \mathbb{R}^{1 \times D_{n_r}}$ to predict the mean-pooled hidden states of the teacher transformer blocks, denoted as $\bar{C}_t \in \mathbb{R}^{1 \times D_{n_r}}$. The global loss L_g is formulated as:

$$L_g = \left\| C_s^{(N)} - \bar{C}_t \right\|_2^2 \quad (5)$$

During the training process, the student CAT encoder f_θ , the projector g_ϕ and the representation alignment head p_δ are trainable, while the teacher CAT encoder $f_{\bar{\theta}}$ is frozen. The teacher CAT encoder is updated using an Exponential Moving Average (EMA) strategy with a linearly increasing momentum coefficient τ . This process is described by the following equation:

$$\bar{\theta} \leftarrow \tau\theta + (1 - \tau)\bar{\theta} \quad (6)$$

4 Experiments

4.1 Datasets

We conduct self-supervised pre-training on the AS-2M subset of AudioSet [Gemmeke *et al.*, 2017], utilizing approximately 1.9 million audio clips without labels. For downstream evaluation, we benchmark our model on three datasets: AudioSet

Table 1: **Comparison of supervised and self-supervised pre-trained models.** Pre-training data abbreviations: ImageNet (IN), AudioSet (AS) and LibriSpeech (LS). TA and TI denote the 128K text-audio pairs and 400M text-image pairs for CLAP and CLIP pre-training, respectively.

Model	#Param	Pre-training Data	AS-2M mAP(%)	AS-20K mAP(%)	ESC-50 Acc(%)	SPCV2 Acc(%)
PANN [Kong <i>et al.</i> , 2020]	81M	-	43.1	27.8	83.3	61.8
PSLA [Gong <i>et al.</i> , 2021b]	14M	IN	44.4	31.9	-	96.3
AST [Gong <i>et al.</i> , 2021a]	86M	IN	45.9	34.7	88.7	98.1
MBT [Nagrani <i>et al.</i> , 2021]	86M	IN-21K	44.3	31.3	-	-
PassT [Koutini <i>et al.</i> , 2022]	86M	IN	47.1	-	96.8	-
HTS-AT [Chen <i>et al.</i> , 2022a]	31M	IN	47.1	-	97.0	98.0
Wav2CLIP [Wu <i>et al.</i> , 2022]	74M	TI+AS	-	-	86.0	-
AudioCLIP [Guzhov <i>et al.</i> , 2022]	93M	TI+AS	25.9	-	96.7	-
Conformer [Srivastava <i>et al.</i> , 2022]	88M	AS	41.1	-	88.0	-
SS-AST [Gong <i>et al.</i> , 2022]	89M	AS+LS	-	31.0	88.8	98.0
MAE-AST [Baade <i>et al.</i> , 2022]	86M	AS+LS	-	30.6	90.0	97.9
MSM-MAE [Niizumi <i>et al.</i> , 2022]	86M	AS	-	-	85.6	87.3
data2vec [Baevski <i>et al.</i> , 2022]	94M	AS	-	34.5	-	-
Audio-MAE [Huang <i>et al.</i> , 2022]	86M	AS	47.3	37.1	94.1	98.3
BEATs _{iter3} [Chen <i>et al.</i> , 2022b]	90M	AS	48.0	38.3	95.6	98.3
BEATs _{iter3+} [Chen <i>et al.</i> , 2022b]	90M	AS	48.6	38.9	98.1	98.1
CLAP [Wu <i>et al.</i> , 2023]	86M	TA	46.9	36.7	96.7	96.8
MaskSpec [Chong <i>et al.</i> , 2023]	86M	AS	47.1	32.3	89.6	97.7
A-JEPA [Fei <i>et al.</i> , 2023]	86M	AS	48.6	38.4	96.3	98.5
EAT [Chen <i>et al.</i> , 2024]	88M	AS	48.6	40.2	95.9	98.3
M2D-CLAP [Niizumi <i>et al.</i> , 2024b]	86M	TA+AS	48.5	41.8	97.4	98.3
ATST-Frame [Li <i>et al.</i> , 2024]	86M	AS	48.0	39.0	-	98.1
ATST-Clip [Li <i>et al.</i> , 2024]	86M	AS	45.2	37.9	-	98.0
ASiT [Ahmed <i>et al.</i> , 2024]	86M	AS	48.0	38.6	95.3	98.9
ASDA [Wang <i>et al.</i> , 2025]	93M	AS	49.0	41.5	96.1	98.3
Ours						
CAT	91M	AS	50.2	47.8	98.6	98.3

(fine-tuning on both the full AS-2M and the balanced AS-20K subsets), ESC-50 [Piczak, 2015], and Speech Commands V2 (SPC-2) [Warden, 2018]. We report mean Average Precision (mAP) for AudioSet tasks. For ESC-50, we assess out-of-domain generalization using standard 5-fold cross-validation accuracy. Finally, we evaluate speech understanding capabilities on SPC-2, employing the official training/test splits and reporting classification accuracy.

More details are provided in Appendix.

4.2 Experimental Setup

Input Processing To extract the input audio spectrogram, each audio clip is first resampled to 16 kHz. We then compute the Mel-frequency spectrogram using 128 filter banks, a 25-ms Hanning window, and a 10-ms frame shift. For the masking strategy, we adopt the Inverse Block Masking proposed in Data2Vec 2.0 [Baevski *et al.*, 2023], with a mask ratio of 80%. This strategy begins by masking all patches and then iteratively unmasks blocks of adjacent patches until the desired masking ratio is reached. For data augmentation, we create four distinct masks for each audio clip.

Model Architecture The CAT encoder begins with the Multi-resolution Block, which progressively projects input patches into a 768-dimensional feature space via convolutional

layers. This is followed by a Transformer backbone consisting of 12 layers with a hidden dimension of 768 and 12 attention heads. To ensure fair comparisons, we adjust the number of transformer layers in specific ablation settings to maintain consistent parameter counts with baselines. The student projector consists of five strided convolutional layers followed by a linear projection.

Training Details Pre-training is conducted on AS-2M for 400k steps with a batch size of 96 using 2 NVIDIA H200 GPUs, taking approximately 3 days. We use the Adam optimizer ($\beta_1 = 0.9, \beta_2 = 0.95$) with a cosine annealing scheduler [Loshchilov and Hutter, 2017], a peak learning rate of 5×10^{-4} , and a warm-up phase of 53,333 steps. The global loss weight λ_1 is set to 1.0. For supervised fine-tuning, models are trained for 300k steps on AS-2M and 40k steps on other datasets.

More details are provided in Appendix.

4.3 Main Results

We compare CAT with state-of-the-art (SOTA) baselines across three distinct training paradigms: supervised learning (e.g., AST, HTS-AT), contrastive learning (e.g., CLAP), and self-supervised learning (e.g., Audio-MAE, EAT, BEATs). The comprehensive results are reported in Table 1. On Au-

dioSet, CAT establishes a new SOTA result, achieving 50.2 mAP on AS-2M and 47.8 mAP on AS-20K. Notably, it outperforms the leading bootstrap method ASDA by +1.2 mAP on AS-2M and by a remarkable +6.3 mAP on the smaller AS-20K dataset. These results validate that our Multi-resolution Block effectively captures complex hierarchies, while Representation Regularization acts as a semantic scaffold to significantly boost data efficiency. CAT also demonstrates superior generalization, setting a new benchmark on ESC-50 with 98.6% accuracy and maintaining competitive performance on Speech Commands V2 (98.3%), confirming its robustness across diverse audio and speech domains.

4.4 Pre-training Efficiency

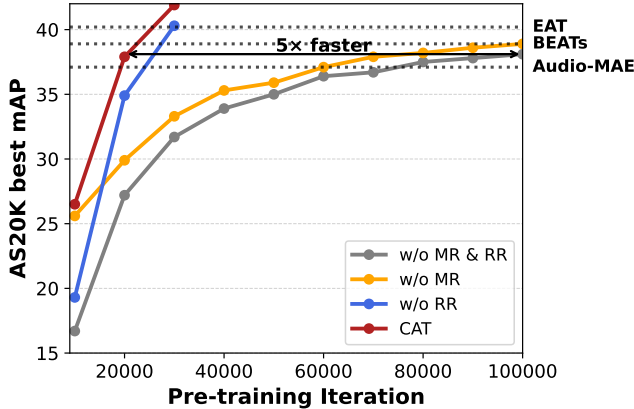


Figure 3: **CAT Pre-training Convergence Performance.** “w/o MR” denotes the model using a vanilla patch embedding instead of the multi-resolution block, while “w/o RR” denotes the model without representation regularization. The x-axis indicates the pre-training step (showing only the early phase), while the y-axis shows the best mAP on AS-20K after supervised fine-tuning with the corresponding checkpoint. For ease of comparison, the best reported performances of EAT, BEATs and Audio-MAE models are indicated by horizontal dashed lines in the plot.

We analyze the convergence behavior of CAT in Figure 3. The results demonstrate that both the architectural design and the regularization objective contribute significantly to training efficiency. First, the Multi-resolution Block introduces effective structural inductive biases. Compared to the single-resolution baseline (“w/o MR”), this hierarchical design enables the model to capture discriminative audio patterns much more rapidly in the early training stages. Second, Representation Regularization acts as a powerful accelerator. As shown by the comparison with the “w/o RR” variant, incorporating external semantic guidance induces a significantly steeper learning curve. This confirms that guiding the student with a mature teacher effectively mitigates the slow “cold-start” phase inherent in bootstrapping from scratch. By combining these two innovations, CAT achieves a competitive 37.9% mAP on AS-20K within just 20,000 iterations. In contrast, baseline methods typically require 100,000 iterations to reach comparable performance. This translates to a 5 \times improvement in pre-training efficiency, significantly reducing

the computational cost of developing high-performance audio models.

4.5 Ablation Study

Table 2: **Component-wise ablation.** “w/o MR” denotes the model using a vanilla patch embedding instead of the multi-resolution block, while “w/o RR” denotes the model without representation regularization.

Model	AS2M	AS20K	ECS50	SPCV2
CAT	50.2	47.8	98.6	98.3
w/o MR	50.0	47.3	98.6	98.1
w/o RR	49.4	41.6	96.5	98.3
w/o MR&RR	48.9	40.6	96.5	98.0

Ablation Study of Component

We perform a component-wise ablation in Table 2 to isolate the contributions of the Multi-resolution (MR) Block and Representation Regularization (RR). The results highlight the critical role of Representation Regularization in boosting data efficiency. Removing this component (“w/o RR”) results in a drastic performance drop, particularly on the data-limited AS-20K benchmark, where mAP plummets from 47.8% to 41.6%. This substantial 6.2% gap confirms our hypothesis: external semantic guidance acts as a crucial scaffold, enabling the model to learn high-quality representations even when pre-training data is limited. Similarly, the Multi-resolution Block proves indispensable for capturing fine-grained audio patterns. Replacing our hierarchical block with a standard patch embedding (“w/o MR”) consistently degrades performance across both AS-2M and AS-20K datasets. Ultimately, the full CAT model achieves the best performance, demonstrating that hierarchical feature extraction and generative semantic regularization are complementary mechanisms that jointly drive the model’s state-of-the-art results.

Ablation Study of Multi-Resolution Block

Table 3: **Ablation of Resolution Configurations.** The multi resolution column indicates the set of resolution hyperparameters $\{r_1, r_2, \dots, r_{n_r}\}$ used in the multi-resolution block. The transformer #layer column specifies the number of Transformer blocks.

Multi Resolution	Transformer #Layer	#Param	AS-20K mAP(%)
{16}	12	88M	40.2
{4,16}	12	100M	41.4
{8,16}	12	93M	41.6
{4,8,16}	11	91M	41.6
{4,8,16,32}	12	128M	38.1

The number of resolution blocks and the patch resolution adopted for these blocks are the most important parameters for the multi-resolution block configuration. Table 3 investigates the effects of different resolution block configurations within the multi-resolution block. Since all features extracted

from the different resolution blocks are downsampled to the same shape as the final resolution block via the subsequent downSample convolution block, the final resolution determines the sequence length of the features input to the subsequent transformer blocks. For fair comparison, the final resolution in most settings is set to 16, following existing works. Extremely large resolution sets (e.g., $\{4, 8, 16, 32\}$) significantly reduce the feature length, leading to suboptimal performance. It is worth mentioning that the single-resolution setting $\{16\}$ essentially degenerates to the baseline model, but with an additional convolution block appended. As demonstrated in Table 3, the results indicate that both the set of resolution hyperparameters r_i and the model depth significantly impact performance. The setting $\{4, 8, 16\}$, using 3 resolution blocks with resolutions 4, 8, and 16 separately, achieves the best performance. We adopt $\{4, 8, 16\}$ as our default setting, as it achieves performance comparable to the $\{8, 16\}$ setting with fewer model parameters. It is worth noting that for the $\{4, 8, 16\}$ setting, one transformer layer is removed to ensure the model size remains comparable to that of existing methods.

Ablation Study of Representation Regularization

Table 4: **Ablation of Target representation.** The Model column indicates the model from which representations are extracted. We utilize the hidden states from the last layer for representation regularization. The first row is the baseline without using representation regularization for comparison.

Model	AS2M	AS20K	ECS50	SPCV2	Avg.
-	48.6	40.2	95.9	98.3	70.8
CLAP	50.0	47.3	98.6	98.3	73.6
AST	50.0	46.6	98.7	98.1	73.4
AudioMAE	50.6	46.6	98.4	97.9	73.4

Target representation Source. To investigate how different types of representations affect the training process and identify the optimal target representation, we conduct ablation studies using representations extracted from models trained in different manners. We find that representation regularization generalizes well, as shown in Table 4. For models pre-trained with representation regularization, we observe substantial improvements over the baseline on general audio related metrics, but a slight drop on SPCV2 (except for the model guided by CLAP features). We suspect that other representations are pre-trained only on audio data, which renders them strong at audio understanding but limits their generalization to speech understanding. CLAP is used as the target representation unless otherwise mentioned in the following experiments, as it yields the best overall performance.

Representation Regularization Layer. The choice of which student transformer block to align with the CLAP representation significantly impacts performance. Applying the representation regularization loss L_r to the CLS token from the final student block yields the best result. Performance gradually degrades when the alignment is applied to earlier student blocks. This trend indicates that the feature representations within the student model become progressively

Table 5: **Component-wise analysis.** The aligned layer d specifies which student transformer block is aligned, the regularization loss weight is λ_2 for regularization loss term L_r .

Aligned Layer	Regularization Loss Weight	Objective	AS-20K mAP(%)
12	1.0	MSE	47.3
10	1.0	MSE	47.1
8	1.0	MSE	46.6
12	5.0	MSE	47.1
12	1.0	MSE	47.3
12	0.1	MSE	45.8
12	1.0	MSE	47.3
12	1.0	CE	42.4
12	1.0	l_1	46.8
12	1.0	cosine	47.2

more refined and semantically meaningful through the layers. Aligning the high-level representations from student blocks with the powerful CLAP embedding T provides a more effective and stable training signal for the overall model.

Loss Weight. The weighting coefficient λ_2 for L_r balances its influence against other loss terms. A weight of 1.0 yields the optimal result. Deviating from this value—either increasing to 5.0 or decreasing to 0.1—leads to a performance drop. This confirms that representation regularization plays a crucial role. An overly strong weight may distort the primary pre-training task, while an overly weak one provides insufficient guidance.

Objective Function. The choice of the objective function is critical for effective feature alignment. The Mean Squared Error (MSE) loss achieves the best performance, significantly outperforming the Cross-Entropy (CE) loss and marginally surpassing both the l_1 loss and the Cosine similarity loss.

Audio Caption Understanding

To further assess the semantic richness of the learned representations, we evaluate CAT and baseline systems on the Audio Captioning task and results are provided in Appendix.

5 Conclusion

In this work, we proposed the Convolutional Audio Transformer (CAT) to address the limitations of single-granularity processing and inefficient training in bootstrap-based SSL. We introduced a Multi-resolution Block to capture hierarchical audio structures and leveraged Representation Regularization, which is inspired by generative modeling, to guide the learning process with external semantic priors. By treating masked prediction as an implicit generative task, our approach significantly accelerates convergence while enhancing feature quality. Experiments confirm that CAT establishes new state-of-the-art performance on AudioSet and ESC-50 while achieving 5x faster convergence than existing baselines, validating the potential of bridging self-supervised learning with generative guidance for efficient audio understanding.

Ethical Statement

There are no ethical issues. All data used in this work were collected and processed in accordance with relevant ethical guidelines and licensing terms.

References

[Ahmed *et al.*, 2024] Sara Atito Ali Ahmed, Muhammad Awais, Wenwu Wang, Mark D Plumbley, and Josef Kittler. ASiT: Local-global audio spectrogram vision transformer for event classification. *IEEE/ACM Transactions on Audio, Speech, and Language Processing*, 32:3684–3693, 2024.

[Anderson *et al.*, 2016] Peter Anderson, Basura Fernando, Mark Johnson, and Stephen Gould. Spice: Semantic propositional image caption evaluation. In *European conference on computer vision*, pages 382–398. Springer, 2016.

[Baade *et al.*, 2022] Alan Baade, Puyuan Peng, and David Harwath. MAE-AST: Masked autoencoding audio spectrogram transformer. In *Proc. Interspeech 2022*, pages 2438–2442, 2022.

[Baevski *et al.*, 2022] Alexei Baevski, Wei-Ning Hsu, Qiantong Xu, Arun Babu, Jiatao Gu, and Michael Auli. Data2vec: A general framework for self-supervised learning in speech, vision and language. In *International conference on machine learning*, pages 1298–1312. PMLR, 2022.

[Baevski *et al.*, 2023] Alexei Baevski, Arun Babu, Wei-Ning Hsu, and Michael Auli. Efficient self-supervised learning with contextualized target representations for vision, speech and language. In *International Conference on Machine Learning*, pages 1416–1429. PMLR, 2023.

[Banerjee and Lavie, 2005] Satanjeev Banerjee and Alon Lavie. Meteor: An automatic metric for mt evaluation with improved correlation with human judgments. In *Proceedings of the acl workshop on intrinsic and extrinsic evaluation measures for machine translation and/or summarization*, pages 65–72, 2005.

[Chen *et al.*, 2022a] Ke Chen, Xingjian Du, Bilei Zhu, Zejun Ma, Taylor Berg-Kirkpatrick, and Shlomo Dubnov. HTS-AT: A hierarchical token-semantic audio transformer for sound classification and detection. In *ICASSP 2022-2022 IEEE International Conference on Acoustics, Speech and Signal Processing (ICASSP)*, pages 646–650. IEEE, 2022.

[Chen *et al.*, 2022b] Sanyuan Chen, Yu Wu, Chengyi Wang, Shujie Liu, Daniel Tompkins, Zhuo Chen, Wanxiang Che, Xiangzhan Yu, and Furu Wei. BEATs: Audio pre-training with acoustic tokenizers. *Proc. ICML*, 2022.

[Chen *et al.*, 2024] Wenxi Chen, Yuzhe Liang, Ziyang Ma, Zhisheng Zheng, and Xie Chen. EAT: Self-supervised pre-training with efficient audio transformer. In *IJCAI*, 2024.

[Chen *et al.*, 2025a] Hesen Chen, Junyan Wang, Zhiyu Tan, and Hao Li. SARA: Structural and adversarial representation alignment for training-efficient diffusion models. *arXiv preprint arXiv:2503.08253*, 2025.

[Chen *et al.*, 2025b] Wenxi Chen, Ziyang Ma, Xiquan Li, Xuenan Xu, Yuzhe Liang, Zhisheng Zheng, Kai Yu, and Xie Chen. SLAM-AAC: Enhancing audio captioning with paraphrasing augmentation and CLAP-refine through LLMs. In *ICASSP 2025-2025 IEEE International Conference on Acoustics, Speech and Signal Processing (ICASSP)*, pages 1–5. IEEE, 2025.

[Chong *et al.*, 2023] Dading Chong, Helin Wang, Peilin Zhou, and Qingcheng Zeng. Masked spectrogram prediction for self-supervised audio pre-training. In *ICASSP 2023-2023 IEEE International Conference on Acoustics, Speech and Signal Processing (ICASSP)*, pages 1–5. IEEE, 2023.

[Drossos *et al.*, 2020] Konstantinos Drossos, Samuel Lippling, and Tuomas Virtanen. Clotho: An audio captioning dataset. In *ICASSP 2020-2020 IEEE International Conference on Acoustics, Speech and Signal Processing (ICASSP)*, pages 736–740. IEEE, 2020.

[Fei *et al.*, 2023] Zhengcong Fei, Mingyuan Fan, and Junshi Huang. A-JEPA: Joint-embedding predictive architecture can listen. *arXiv preprint arXiv:2311.15830*, 2023.

[Gemmeke *et al.*, 2017] Jort F Gemmeke, Daniel PW Ellis, Dylan Freedman, Aren Jansen, Wade Lawrence, R Channing Moore, Manoj Plakal, and Marvin Ritter. Audio set: An ontology and human-labeled dataset for audio events. In *2017 IEEE International Conference on Acoustics, Speech and Signal Processing (ICASSP)*, pages 776–780. IEEE, 2017.

[Gong *et al.*, 2021a] Yuan Gong, Yu-An Chung, and James Glass. AST: Audio spectrogram transformer. *Interspeech 2021*, 2021.

[Gong *et al.*, 2021b] Yuan Gong, Yu-An Chung, and James Glass. PSLA: Improving audio tagging with pretraining, sampling, labeling, and aggregation. *IEEE/ACM Transactions on Audio, Speech, and Language Processing*, 29:3292–3306, 2021.

[Gong *et al.*, 2022] Yuan Gong, Cheng-I Lai, Yu-An Chung, and James Glass. SSAST: Self-supervised audio spectrogram transformer. In *Proceedings of the AAAI Conference on Artificial Intelligence*, volume 36, pages 10699–10709, 2022.

[Guzhov *et al.*, 2022] Andrey Guzhov, Federico Raue, Jörn Hees, and Andreas Dengel. AudioCLIP: Extending CLIP to image, text and audio. In *ICASSP 2022-2022 IEEE International Conference on Acoustics, Speech and Signal Processing (ICASSP)*, pages 976–980. IEEE, 2022.

[He *et al.*, 2022] Kaiming He, Xinlei Chen, Saining Xie, Yanghao Li, Piotr Dollár, and Ross Girshick. Masked autoencoders are scalable vision learners. In *Proceedings of the IEEE/CVF conference on Computer Vision and Pattern Recognition*, pages 16000–16009, 2022.

[Ho *et al.*, 2020] Jonathan Ho, Ajay Jain, and Pieter Abbeel. Denoising diffusion probabilistic models. *Advances in Neural Information Processing Systems*, 33:6840–6851, 2020.

[Hu *et al.*, 2022] Edward J Hu, Yelong Shen, Phillip Wallis, Zeyuan Allen-Zhu, Yuanzhi Li, Shean Wang, Lu Wang, Weizhu Chen, et al. Lora: Low-rank adaptation of large language models. *ICLR*, 1(2):3, 2022.

[Huang *et al.*, 2016] Gao Huang, Yu Sun, Zhuang Liu, Daniel Sedra, and Kilian Q Weinberger. Deep networks with stochastic depth. In *European Conference on Computer Vision*, pages 646–661. Springer, 2016.

[Huang *et al.*, 2022] Po-Yao Huang, Hu Xu, Juncheng Li, Alexei Baevski, Michael Auli, Wojciech Galuba, Florian Metze, and Christoph Feichtenhofer. Masked autoencoders that listen. *Advances in Neural Information Processing Systems*, 35:28708–28720, 2022.

[Kim *et al.*, 2019] Chris Dongjoo Kim, Byeongchang Kim, Hyunmin Lee, and Gunhee Kim. Audiocaps: Generating captions for audios in the wild. In *Proceedings of the 2019 Conference of the North American Chapter of the Association for Computational Linguistics: Human Language Technologies, Volume 1 (Long and Short Papers)*, pages 119–132, 2019.

[Kong *et al.*, 2020] Qiuqiang Kong, Yin Cao, Turab Iqbal, Yuxuan Wang, Wenwu Wang, and Mark D Plumley. PANNs: Large-scale pretrained audio neural networks for audio pattern recognition. *IEEE/ACM Transactions on Audio, Speech, and Language Processing*, 28:2880–2894, 2020.

[Koutini *et al.*, 2022] Khaled Koutini, Jan Schlüter, Hamid Eghbal-zadeh, and Gerhard Widmer. Efficient training of audio transformers with patchout. In *Proc. Interspeech 2022*, pages 2753–2757, 2022.

[Lee *et al.*, 2025] Jaa-Yeon Lee, Byunghee Cha, Jeongsol Kim, and Jong Chul Ye. Aligning text to image in diffusion models is easier than you think. *arXiv preprint arXiv:2503.08250*, 2025.

[Li *et al.*, 2024] Xian Li, Nian Shao, and Xiaofei Li. Self-supervised audio teacher-student transformer for both clip-level and frame-level tasks. *IEEE/ACM Transactions on Audio, Speech, and Language Processing*, 32:1336–1351, 2024.

[Liu *et al.*, 2017] Siqi Liu, Zhenhai Zhu, Ning Ye, Sergio Guadarrama, and Kevin Murphy. Improved image captioning via policy gradient optimization of spider. In *Proceedings of the IEEE international conference on computer vision*, pages 873–881, 2017.

[Loshchilov and Hutter, 2017] Ilya Loshchilov and Frank Hutter. SGDR: Stochastic gradient descent with warm restarts. In *International Conference on Learning Representations*, 2017.

[Loshchilov and Hutter, 2019] Ilya Loshchilov and Frank Hutter. Decoupled weight decay regularization. In *International Conference on Learning Representations*, 2019.

[Martín-Morató and Mesaros, 2021] Irene Martín-Morató and Annamaria Mesaros. What is the ground truth? reliability of multi-annotator data for audio tagging. In *2021 29th European Signal Processing Conference (EUSIPCO)*, pages 76–80. IEEE, 2021.

[Mei *et al.*, 2024] Xinhao Mei, Chutong Meng, Haohe Liu, Qiuqiang Kong, Tom Ko, Chengqi Zhao, Mark D Plumley, Yuexian Zou, and Wenwu Wang. Wavcaps: A chatgpt-assisted weakly-labelled audio captioning dataset for audio-language multimodal research. *IEEE/ACM Transactions on Audio, Speech, and Language Processing*, 32:3339–3354, 2024.

[Nagrani *et al.*, 2021] Arsha Nagrani, Shan Yang, Anurag Arnab, Aren Jansen, Cordelia Schmid, and Chen Sun. Attention bottlenecks for multimodal fusion. *Advances in Neural Information Processing Systems*, 34:14200–14213, 2021.

[Niizumi *et al.*, 2022] Daisuke Niizumi, Daiki Takeuchi, Yasunori Ohishi, Noboru Harada, and Kunio Kashino. Masked spectrogram modeling using masked autoencoders for learning general-purpose audio representation. In *HEAR: Holistic Evaluation of Audio Representations*, pages 1–24. PMLR, 2022.

[Niizumi *et al.*, 2024a] Daisuke Niizumi, Daiki Takeuchi, Yasunori Ohishi, Noboru Harada, and Kunio Kashino. Masked modeling duo: Towards a universal audio pre-training framework. *IEEE/ACM Transactions on Audio, Speech, and Language Processing*, 32:2391–2406, 2024.

[Niizumi *et al.*, 2024b] Daisuke Niizumi, Daiki Takeuchi, Yasunori Ohishi, Noboru Harada, Masahiro Yasuda, Shunsuke Tsubaki, and Keisuke Imoto. M2D-CLAP: Masked modeling duo meets CLAP for learning general-purpose audio-language representation. In *Proc. Interspeech 2024*, pages 57–61, 2024.

[Niu *et al.*, 2025] Zhikang Niu, Shujie Hu, Jeongsoo Choi, Yushen Chen, Peining Chen, Pengcheng Zhu, Yunting Yang, Bowen Zhang, Jian Zhao, Chunhui Wang, et al. Semantic-VAE: Semantic-alignment latent representation for better speech synthesis. *arXiv preprint arXiv:2509.22167*, 2025.

[Oquab *et al.*, 2024] Maxime Oquab, Timothée Darcet, Théo Moutakanni, Huy V Vo, Marc Szafraniec, Vasil Khalidov, Pierre Fernandez, Daniel HAZIZA, Francisco Massa, Alaeldin El-Nouby, et al. DINOv2: Learning robust visual features without supervision. *Transactions on Machine Learning Research*, 2024.

[Park *et al.*, 2019] Daniel S Park, William Chan, Yu Zhang, Chung-Cheng Chiu, Barret Zoph, Ekin D Cubuk, and Quoc V Le. SpecAugment: A simple data augmentation method for automatic speech recognition. In *Proc. Interspeech 2019*, pages 2613–2617, 2019.

[Piczak, 2015] Karol J Piczak. ESC: Dataset for environmental sound classification. In *Proceedings of the 23rd ACM international conference on Multimedia*, pages 1015–1018, 2015.

[Singh *et al.*, 2025] Jaskirat Singh, Xingjian Leng, Zongze Wu, Liang Zheng, Richard Zhang, Eli Shechtman, and Saining Xie. What matters for representation alignment: Global information or spatial structure? *arXiv preprint arXiv:2512.10794*, 2025.

[Song *et al.*, 2021] Yang Song, Jascha Sohl-Dickstein, Diederik P Kingma, Abhishek Kumar, Stefano Ermon, and Ben Poole. Score-based generative modeling through stochastic differential equations. In *International Conference on Learning Representations*, 2021.

[Srivastava *et al.*, 2014] Nitish Srivastava, Geoffrey Hinton, Alex Krizhevsky, Ilya Sutskever, and Ruslan Salakhutdinov. Dropout: a simple way to prevent neural networks from overfitting. *The journal of machine learning research*, 15(1):1929–1958, 2014.

[Srivastava *et al.*, 2022] Sangeeta Srivastava, Yun Wang, Andros Tjandra, Anurag Kumar, Chunxi Liu, Kritika Singh, and Yatharth Saraf. Conformer-based self-supervised learning for non-speech audio tasks. In *ICASSP 2022-2022 IEEE International Conference on Acoustics, Speech and Signal Processing (ICASSP)*, pages 8862–8866. IEEE, 2022.

[Vedantam *et al.*, 2015] Ramakrishna Vedantam, C Lawrence Zitnick, and Devi Parikh. Cider: Consensus-based image description evaluation. In *Proceedings of the IEEE conference on computer vision and pattern recognition*, pages 4566–4575, 2015.

[Wang *et al.*, 2025] Junyu Wang, Tianrui Wang, Meng Ge, Longbiao Wang, and Jianwu Dang. ASDA: Audio spectrogram differential attention mechanism for self-supervised representation learning. *Interspeech 2025*, 2025.

[Warden, 2018] Pete Warden. Speech commands: A dataset for limited-vocabulary speech recognition. *arXiv preprint arXiv:1804.03209*, 2018.

[Wu *et al.*, 2022] Ho-Hsiang Wu, Prem Seetharaman, Kundan Kumar, and Juan Pablo Bello. Wav2CLIP: Learning robust audio representations from CLIP. In *ICASSP 2022-2022 IEEE International Conference on Acoustics, Speech and Signal Processing (ICASSP)*, pages 4563–4567. IEEE, 2022.

[Wu *et al.*, 2023] Yusong Wu, Ke Chen, Tianyu Zhang, Yuchen Hui, Taylor Berg-Kirkpatrick, and Shlomo Dubnov. Large-scale contrastive language-audio pretraining with feature fusion and keyword-to-caption augmentation. In *ICASSP 2023-2023 IEEE International Conference on Acoustics, Speech and Signal Processing (ICASSP)*, pages 1–5. IEEE, 2023.

[Yu *et al.*, 2025] Sihyun Yu, Sangkyung Kwak, Huiwon Jang, Jongheon Jeong, Jonathan Huang, Jinwoo Shin, and Saining Xie. Representation alignment for generation: Training diffusion transformers is easier than you think. In *The Thirteenth International Conference on Learning Representations*, 2025.

[Zhang *et al.*, 2018] Hongyi Zhang, Moustapha Cisse, Yann N Dauphin, and David Lopez-Paz. mixup: Beyond empirical risk minimization. In *International Conference on Learning Representations*, 2018.

[Zhou *et al.*, 2022] Zelin Zhou, Zhiling Zhang, Xuenan Xu, Zeyu Xie, Mengyue Wu, and Kenny Q Zhu. Can audio captions be evaluated with image caption metrics?

In *ICASSP 2022-2022 IEEE International Conference on Acoustics, Speech and Signal Processing (ICASSP)*, pages 981–985. IEEE, 2022.

A Datasets Detail

We utilized AudioSet for self-supervised pre-training and evaluated the learned representations on AudioSet, ESC-50, and Speech Commands V2 through supervised fine-tuning. The details of these datasets are as follows:

AudioSet AudioSet [Gemmeke *et al.*, 2017] is a large-scale audio event dataset consisting of approximately 2 million 10-second audio clips extracted from YouTube videos, covering 527 distinct audio event classes. The dataset is organized into three subsets: the unbalanced training subset (AS-2M), the balanced training subset (AS-20K), and the evaluation subset. We use the huggingface version¹, which contains 20,550/22,160 of the balanced training subset, 1,913,637/2,041,789 of the unbalanced training subset, and 18,887/20,371 of the evaluation subset. In this work, we use the AS-2M subset for pre-training, utilizing only the audio data without labels. For downstream evaluation, we conduct supervised fine-tuning on both AS-2M and AS-20K and report the mean Average Precision (mAP) on the official evaluation subset.

Environmental Sound Classification (ESC-50) The ESC-50 dataset [Piczak, 2015] is a widely used benchmark for environmental sound classification, comprising 2,000 labeled audio clips. It serves as an out-of-domain dataset to evaluate the generalization capability of the model. Following the experimental settings of EAT and M2D-CLAP, we employ a 5-fold cross-validation strategy and report the average accuracy (Acc) as the evaluation metric.

Speech Commands (SPCV2) Speech Commands V2 [Warden, 2018] is a keyword spotting dataset consisting of 105,829 one-second audio recordings of spoken English words. The dataset is partitioned into training, validation, and test sets, containing 84,843, 9,981 and 11,005 samples, respectively. During fine-tuning, the model is trained on the training set, and classification accuracy (Acc) on the test set is used as the performance metric.

B Baseline Systems Detail

To validate the effectiveness of our proposed method, we compare CAT with several representative state-of-the-art audio understanding models. These baselines cover three distinct training paradigms: supervised pretraining, contrastive learning pretraining, and self-supervised learning.

B.1 Supervised Pretraining

AST [Gong *et al.*, 2021a] is a representative supervised learning model. It is the first attention-based model to introduce the Vision Transformer (ViT) architecture to the audio domain. AST processes audio spectrograms as a sequence of patch embeddings. During pre-training, it relies on large-scale supervised datasets (e.g., ImageNet for initialization followed by AudioSet) to learn audio representations. While

¹<https://huggingface.co/datasets/confit/audioset-quiqiangkong>

Table 6: CAT pre-training and fine-tuning hyper-parameters.

Hyperparameters	Pre-Training		Fine-Tuning		
	AS-2M	AS-2M	AS-20K	ESC-50	SPCV2
Optimizer	AdamW [Loshchilov and Hutter, 2019]				
Optimizer Momentum	$\beta_1 = 0.9, \beta_2 = 0.95$				
Weight Decay	0.05				
Learning Rate Schedule	Cosine [Loshchilov and Hutter, 2017]				
Peak Learning Rate	0.0005	0.00005	0.00005	0.00005	0.0002
Minimum Learning Rate			0.000001		
Steps	400K	300K	40K	4K	40K
Warm-up steps	53K	30K	4K	400	4K
Batch size	12	96	48	48	256
Clone batch	16			N/A	
Number of GPUs	4			1	
Dropout [Srivastava <i>et al.</i> , 2014]	0.0	0.0	0.0	0.0	0.0
Drop path [Huang <i>et al.</i> , 2016]	0.0	0.1	0.1	0.1	0.1
Weighted Sampling	False	True	False	False	False
Weighted Sampling size	N/A	200K	N/A	N/A	N/A
Roll Augmentation	False	True	True	True	False
Noise Augmentation	False	False	False	False	True
SpecAug [Park <i>et al.</i> , 2019]	N/A	0.2	0.2	0.2	0.1
Mixup [Zhang <i>et al.</i> , 2018]	0.0	0.8	0.8	0.0	0.8
Multi-label	N/A	True	True	False	False
Loss Function	MSE	BCE	BCE	CE	BCE
Dataset Mean for Normalization	-4.268	-4.268	-4.268	-6.627	-6.846
Dataset Std for Normalization	4.569	4.569	4.569	5.359	5.565

effective, AST typically requires large amounts of labeled data, which limits its scalability compared to self-supervised approaches.

B.2 Contrastive Learning Pretraining

CLAP (Contrastive Language-Audio Pretraining) [Wu *et al.*, 2023] represents the contrastive learning paradigm. It consists of dual encoders—one for audio and one for text—trained jointly to align audio representations with their corresponding natural language descriptions. By utilizing large-scale text-audio pairs (e.g., LAION-Audio-630K), CLAP learns robust semantic representations capable of zero-shot transfer. In our work, we not only use CLAP as a strong baseline but also leverage its frozen audio encoder to provide representation regularization for our student model.

B.3 Self-supervised Pretraining

AudioMAE [Huang *et al.*, 2022] is a generative self-supervised learning model. Following the Masked Autoencoder (MAE) framework from the vision domain, AudioMAE masks a high proportion of patches in the input spectrogram and trains the model to reconstruct the missing pixels of the spectrogram from the unmasked patches. This reconstruction-based objective encourages the model to learn local acoustic features and temporal dependencies without requiring labels.

BEATs (Bidirectional Encoder representation from Audio Transformers) [Chen *et al.*, 2022b] is a state-of-the-art

bootstrap-based self-supervised model. It employs an iterative pre-training strategy that utilizes an acoustic tokenizer to generate discrete labels for masked prediction. By learning to predict these discrete acoustic tokens, BEATs achieves superior performance on various audio understanding benchmarks. In our experiments, we compare against the *BEATs_{iter3}* and *BEATs_{iter3+}* variants.

C Model Architecture Detail

In the Multi-resolution Block, patch embedding is performed by a single 2D convolutional layer with a kernel size and stride both set to r_{k+1}/r_k . The number of channels gradually increases from 1 to the final dimension D_{nr} , which is set to 768 to match the Transformer’s hidden dimension. The convolution module within the Multi-resolution Block consists of three sequential layers: a 1×1 convolution for cross-channel information aggregation, followed by a 5×5 convolution with a stride of 1 and padding of 2, and finally another 1×1 convolution. This design maintains both the feature map dimensions and the channel count. The Downsample Block is implemented as a single convolutional layer with a kernel size and stride of r_n/r_k , which downsamples the feature map to match the dimensions of the final layer’s features.

For the Transformer implementation, we use 12 layers for most ablation studies unless otherwise specified. Since we additionally introduce the Multi-Resolution Block, we remove one layer in certain configurations to keep the number of trainable parameters roughly comparable across models,

Table 7: Performance Comparison of Different Models on Audio Captioning Metrics.

Model	METEOR(%)	CIDEr(%)	SPICE(%)	SPIDER(%)	SPIDER-FL(%)	FENSE(%)
Baseline model						
BEATs [Chen <i>et al.</i> , 2022b]	18.5	48.8	13.3	31.0	29.6	50.1
Audio-MAE [Huang <i>et al.</i> , 2022]	15.6	31.2	10.5	20.8	20.8	41.8
AST [Gong <i>et al.</i> , 2021a]	8.9	8.1	4.0	6.0	6.0	21.4
Ours						
CAT	19.8	50.7	14.9	32.8	32.6	53.1

ensuring a fair comparison. The attention module is configured with a hidden size of 768 and 12 heads. Each Transformer block consists of a multi-head attention layer followed by an MLP block, which contains two fully-connected layers with an internal hidden dimension of 4×768 . The projector comprises five convolutional layers followed by a fully-connected layer. The first layer reduces the channel dimension from 768 to 384, while the subsequent four layers maintain this channel size. All convolutional layers use a 5×5 kernel with a padding of 2. Finally, a fully-connected layer projects the features back to the original dimension of 768.

D Training Hyper-Parameters

Additional hyper-parameters used in pre-training using AS-2M and fine-tuning of standard audio SSL benchmark datasets are listed in Table 6.

E Model for Audio Caption

To validate the performance of our model on other audio understanding tasks, we further evaluate the performance of our model and baseline models on the audio captioning task.

E.1 Audio Caption Steup

We align the encoder representations to the language model’s (LM) representation space via a linear projector, which are then directly fed into the subsequent LM for audio captioning tasks. We first pre-train the LM and then conduct supervised fine-tuning (SFT) — with LORA [Hu *et al.*, 2022] applied throughout both stages to facilitate efficient parameter updates. Following the experimental setup of SLAM-AAC [Chen *et al.*, 2025b], we perform pre-training on four datasets: Clotho [Drossos *et al.*, 2020], AudioCaps [Kim *et al.*, 2019], WavCaps [Mei *et al.*, 2024], and MACS [Martín-Morató and Mesaros, 2021]. We adopt paraphrasing augmentation following SLAM-AAC for data augmentation for Clotho dataset, which generates additional semantically consistent captions via back-translation to alleviate data scarcity. The pre-training data includes the training splits of Clotho, AudioCaps, and MACS, as well as the entire WavCaps dataset. Training is conducted with a global batch size of 16, a peak learning rate of 1e-4, a linear decay learning rate schedule with 1,000-iteration warmup, and a total of 100,000 training steps. The model is further fine-tuned on the Clotho training set for 10 epochs (batch size=4, peak learning rate=8e-6), with its audio captioning performance evaluated on the Clotho evaluation split. During inference, our model first

generates multiple candidate captions following SLAM-AAC via beam search with varying beam sizes, then leverages the CLAP model to compute audio-text cosine similarity for each candidate and selects the one with the highest alignment score as the final output.

E.2 Caption Results Analysis

To assess the quality of generated audio captions, we evaluate the caption results using six standard Automated Audio Captioning (AAC) metrics: METEOR [Banerjee and Lavie, 2005], CIDEr [Vedantam *et al.*, 2015], SPICE [Anderson *et al.*, 2016], SPIDER [Liu *et al.*, 2017], SPIDER-FL [Zhou *et al.*, 2022], and FENSE [Zhou *et al.*, 2022]. METEOR evaluates unigram-level precision and recall, while incorporating synonyms and stemming to account for lexical variations. CIDEr quantifies the consensus between generated captions and references through TF-IDF weighted n-gram matching. SPICE takes a semantic graph-based approach, comparing the structural similarity of meaning representations between generated and reference texts. SPIDER offers a balanced assessment by linearly combining CIDEr and SPICE, integrating both syntactic coherence and semantic relevance. Building on SPIDER, SPIDER-FL introduces fluency awareness by incorporating a fluency error detector from FENSE—a BERT-based model fine-tuned on audio captions—penalizing the SPIDER score if the fluency error probability exceeds 90%. FENSE itself provides a holistic evaluation by fusing Sentence-BERT-derived semantic similarity with fluency error detection.

As presented in Table 7, CAT consistently outperforms all baseline models across all reported metrics, demonstrating the superior semantic quality of its learned representations. Specifically, CAT achieves a SPIDER score of 32.8%, surpassing the strong bootstrap-based baseline BEATs by 1.8% and the generative Audio-MAE by a significant margin. Notably, the performance gap is even more pronounced on the SPIDER-FL metric (+3.0% over BEATs), indicating that the captions generated by CAT are not only semantically accurate but also more fluent.

We attribute this superior performance to the proposed Representation Regularization. CAT is explicitly aligned with CLAP, a model pre-trained on audio-text pairs. This alignment effectively injects rich, language-aligned semantic priors into the CAT encoder, enabling it to bridge the modality gap between audio signals and natural language descriptions more effectively than models trained solely on audio reconstruction or classification objectives.